applied sciences

MDPI

Review

Shrinkage-Induced Response of Composite Steel–Concrete Slabs: A State-of-the-Art Review

Md Mahfuzur Rahman and Gianluca Ranzi *

School of Civil Engineering, The University of Sydney, Sydney, NSW 2006, Australia; m.rahman@sydney.edu.au
* Correspondence: gianluca.ranzi@sydney.edu.au

Abstract: Composite steel–concrete slab is a floor typology widely used for building applications. Their design is usually governed by serviceability limit state requirements associated with the time-dependent response of the concrete. In this context, this paper presents a state-of-the-art review of research carried out to date on the long-term behavior of composite steel–concrete slabs. The particularity of this time-dependent response relies on the fact that the concrete cannot dry from the underside of the slab due to the presence of the profiled sheeting while it can dry from its upper surface. In the first part of the paper, a review of the work carried out on the identification of the time-dependent response of the concrete is presented by considering the peculiarities that occur due to the non-symmetric drying condition related to composite slabs. Particular attention is given to shrinkage effects and to the occurrence and influence of the non-uniform shrinkage gradient that develops in this form of construction over time. This is followed by the description and discussion of the experimental work performed on both simply-supported and continuous static configurations of composite slabs. In particular, the work published to date is summarized while highlighting the key parameters of the test samples and of the testing protocols adopted in the experiments. In the last part of the paper, available theoretical and design models proposed for the predictions of the shrinkage-induced behavior of composite slabs are presented and discussed.

Keywords: composite steel–concrete slab; concrete; profiled steel sheeting; shrinkage; time effects

Citation: Rahman, M.M.; Ranzi, G. Shrinkage-Induced Response of Composite Steel–Concrete Slabs: A State-of-the-Art Review. *Appl. Sci.* **2022**, *12*, 223. https://doi.org/10.3390/app12010223

Academic Editor: Dario De Domenico

Received: 30 November 2021
Accepted: 22 December 2021
Published: 27 December 2021

1. Introduction

Composite steel–concrete slabs are widely used for building applications in steel and composite construction. These consist of slabs in which the profiled steel sheeting acts as permanent formwork during casting and, once the concrete hardens, it contributes as external reinforcement [1–6]. The typical layout of a composite slab is shown in Figure 1. The use of composite steel–concrete floors can lead to cost savings and enhance the speed of erection, especially for spans in which the composite slabs can be cast under unpropped conditions. The design of this form of construction is usually governed by serviceability limit state requirements associated with the time-dependent response of the concrete [7–10].

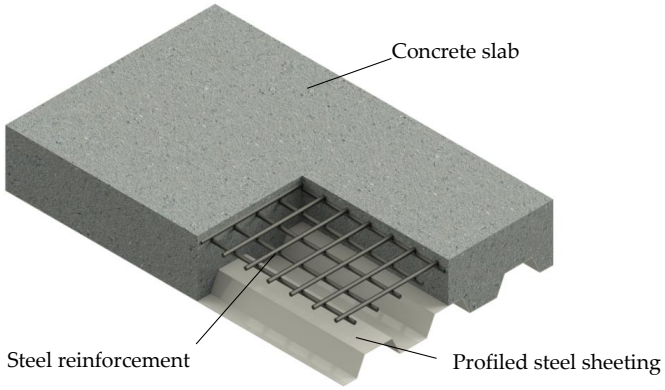

Figure 1. Typical layout of the composite steel–concrete slab.

Extensive research has been carried out on the ultimate response of composite slabs over the last decades, while only limited work has focused on its service response [9,10]. This paper intends to provide a state-of-the-art review of the work carried out to date on the service response of composite slabs influenced by concrete time effects. Particular attention in this paper is devoted to shrinkage effects as recent modelling and experimental work have highlighted the importance of considering the non-symmetric drying conditions produced by the presence of the sheeting due to the inability of the slab to dry from its underside [9,10]. In the first part of the paper, an overview of the research carried out to date to evaluate the time-dependent response of the concrete when cast in a composite slab arrangement is presented. This is followed by a description of the composite slab sample tests performed with different static configurations, i.e., simply-supported and continuous slabs. Particular attention is given to providing the different factors investigated in the different experiments reported in the literature, including the sample geometries, loading conditions, and drying conditions. In the final part of the paper, a description and discussion of available theoretical and design models proposed in the literature are presented and discussed.

2. Time-Dependent Concrete Response in Composite Steel–Concrete Slabs

The time-dependent response of composite slabs is influenced by the presence of the profiled steel sheeting that prevents the concrete to dry from its underside, while enabling it to dry from its upper surface. This non-symmetric exposure drying condition is depicted in Figure 2. In particular, the exposure drying conditions of the top and bottom surfaces are depicted in Figure 2a. Under these conditions, the qualitative profile induced by shrinkage can be described by the non-linear curve shown in Figure 2b that highlights the significant drying that takes place in the vicinity of the top exposed surface. For design purposes, this non-uniform distribution can be simplified into a linearly varying distribution, as also depicted in Figure 2b. This simplification is considered acceptable for routine design [11–13] as long as the service response of the composite slab under consideration is not significantly affected by possible concrete cracking. In fact, in the linearly varying distribution, the self-equilibrating eigenstresses produced by the non-linear profile are not captured and, therefore, neglected.

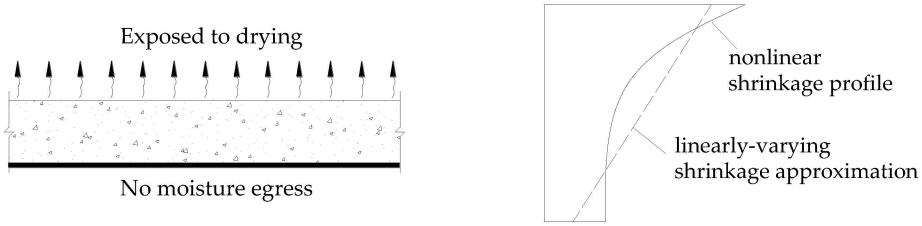

Figure 2. Typical exposure conditions of composite steel–concrete slab and qualitative representations of the shrinkage profiles: (**a**) exposure drying conditions, (**b**) shrinkage profiles.

Extensive work has been carried out in the last decade to characterize the shrinkage response of the concrete induced by the non-symmetric drying conditions. In these works, shrinkage strains were monitored experimentally for small-scaled concrete samples that were cast on different profiled steel sheeting to replicate the actual drying behavior of composite slabs [14–17]. Additional specimens were also cast without the steel sheeting to remove the contribution of its stiffness in the evaluation of the total deformation (that could be regarded as free shrinkage strain measurements) while the barrier to moisture egress was provided to the underside of the slab by the presence of epoxy resin or plastic sheets [14–20]. In these tests, all four sides of the small-scale slab samples were sealed to reproduce the continuity of the slab and the real drying scenario that occurs in a composite

floor. The details of the small-scale slab samples tested to date are summarized in Table 1 and typical experimental setups are depicted in Figure 3.

Table 1. Long-term tests of small-scale specimens to characterize shrinkage effects.

Ref.	Sample ID	f_c' [1] [MPa]	t_0 [1] [Days]	t_k [1] [Days]	L [1] [mm]	b [1] [mm]	D [1] [mm]	Profiled Steel Sheeting	Remarks
[14]	S1	33.7	8	239	900	900	180	None	Solid slab [2]
	S2							None	Solid slab [3]
	S3							Condeck HP® [21]	
	S4							PrimeForm® [22]	
[15]	SS120	27.3	15	210	900	900	120	None	Solid slab [2]
	SS180			120			180		
	SS250			210			250		
	SP120	27.3	15	210	900	900	120	None	Solid slab [3]
	SP180			120			180		
	SP250			210			250		
	PF120	27.3	15	120	900	900	120	PrimeForm® [22]	
	PF180			120			180		
	PF250			120			250		
	CK120	27.3	15	120	900	900	120	Condeck HP® [21]	
	CK180			120			180		
	CK250			120			250		
[16]	SH1	27.3	15	119	900	900	180	None	Solid slab [2]
	SH2							None	Solid slab [3]
	SH3							Condeck HP® [21]	
[17]	1A	34.5	21	322	750	750	150	KF40® [23]	
	1B						150	None	KF40-shaped void [4]
	2A						150	KF70® [23]	
	2B						150	None	KF70-shaped void [4]
	3A						200	KF70® [23]	
	3B						200	None	KF70-shaped void [4]
	4A						300	KF70® [23]	
	4B						300	None	KF70-shaped void [4]
	5A						150	RF55® [23]	
	5B						150	None	RF55-shaped void [4]
[18,20]	ES 120	29.0	28	268	600	600	120	None	Solid slab [5]
	ES 180						180		
[19]	NAC	57.5	28	500	600	510	120	None	Solid slab [5]
	RAC	47.4							

Notes: [1] f_c' is the measured compressive strength of the concrete; t_0 and t_k are the time of first loading and the time at the end of the long-term tests, respectively; L, b, and D are the length, width, and depth of the samples, respectively. [2] Top and bottom surfaces of the samples exposed for drying to the environment. [3] Top surface of the samples exposed for drying to the environment and the bottom surface sealed with plastic. [4] Profiled steel sheeting shaped void formed with polystyrene molds and bottom face of samples covered with an impermeable flexible sealant. [5] Top surface exposed for drying to the environment and the bottom surface sealed with epoxy resin.

Figure 3. Typical experimental setups for measuring the characterization of the shrinkage-induced deformations [14,17].

These samples (such as those depicted in Figure 3) were monitored over time to measure variations in total deformations on both faces of the specimens and, in some instances, through the slab thickness. The strain profiles obtained from these measurements on samples that were sealed on one side by means of epoxy resins or plastic sheets were assumed to approximate a linearly-varying shrinkage profile (see Figure 2b) produced by the free shrinkage strain [14–20]. Examples of these measurements taken at different points in time from casting are depicted in Figure 4 by considering two slab thicknesses of 120 and 250 mm.

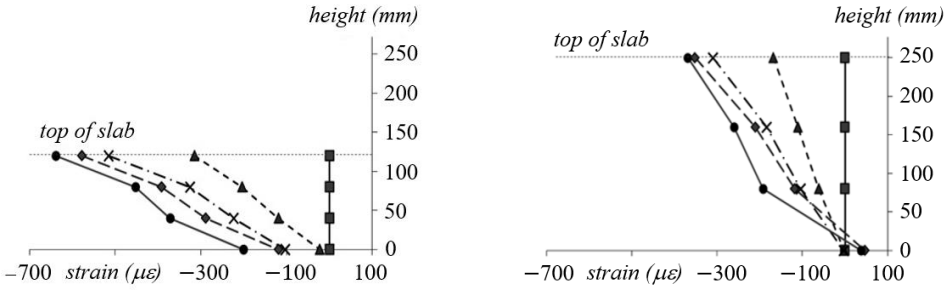

Figure 4. Total deformations measured at 15, 36, 60, 126, and 192 days from casting for samples with different thicknesses and with the top surfaces exposed to dry and bottom surfaces sealed with plastic: (**a**) slab thickness of 120 and (**b**) slab thickness of 250 mm [15].

The small-scale concrete samples [14–20] were monitored over time to evaluate the shrinkage strain variations exhibited through the samples prepared with different cross-sectional geometries (e.g., different steel sheeting profiles and slab thicknesses in the range of 120–300 mm).

As expected, the total strains varied with the slab thickness and decreased with increasing thickness values [15]. In reference [15], the total strains measured at the top surface of the samples that were exposed for drying only from their top surface (i.e., sealed on their bottom surface) were, after 119 days from the day of casting, about 20–30% higher than those noted on the specimens that had symmetric drying conditions (i.e., drying from both top and bottom surfaces). This result has been shown to agree well with other results reported in references [14,16]. The total deformations produced by shrinkage deformations were also reported for samples with trapezoidal profiled sheeting and different slab thicknesses [17].

Extensive research has been carried out to establish experimentally the relationship between the development of shrinkage and variations in moisture content (expressed

in terms of RH) within the concrete and it is beyond the scope of this paper to provide a comprehensive review and reference for this should be made to dedicated textbooks, e.g., [24]. Linear relationships between measured RH values and both autogenous and drying shrinkage deformations were reported in different studies [25–30]. Experimental work was also carried out to identify the interior RH profiles for samples with different dimensions and drying conditions.

Parrott [31,32] measured the interior RH at different depths of 100 mm concrete cube samples sealed on all surfaces except one left for drying to simulate the typical response of a composite slab. In this work, a distinctive RH gradient along the depth of the samples was observed. Other research work was performed on concrete samples with different dimensions, e.g., 100 × 100 × 200 [33], 76 × 76 × 330 [34], 100 × 100 × 300 [35], 200 × 200 × 800 [27,28,35], and 40 × 40 × 160 mm [36]. In all cases, the top surfaces of the samples were exposed for drying, and non-linear RH gradients were observed. Similar results were also noticed in the experimental program on larger samples consisting of 20 slabs with different dimensions of 500 × 500 × 100, 500 × 500 × 150, and 700 × 700 × 200 mm [37,38] and on a concrete slab of 75 × 900 × 6000 mm that was cast on the ground [39,40]. Experiments were also carried out on concrete samples with both top and bottom surfaces exposed to the ambient with symmetric drying conditions applied to the top and bottom surfaces [41–43]. In these cases, measured RH gradients along the depth of the samples were also symmetric. Other work focused on trying to identify the amount of slab thickness that is significantly influenced by environmental conditions and reported actual influence thickness as a function of the samples geometries [44–49].

3. Time-Dependent Responses of Composite Slabs

Experimental work reported in the literature on the long-term testing of composite slabs is presented in the following sections. The published work has been organized according to the static configuration specified in the experiments and the details of these tests are summarized in Tables 2 and 3 for simply-supported and continuous composite specimens, respectively.

3.1. Simply-Supported Composite Slabs

The experimental program involving the long-term testing of simply-supported one-way composite slabs subjected to different loading conditions and prepared with different profiled sheeting were reported in [16,18,50–53]. In this experimental work, all composite slabs increased in deflections over time due to shrinkage and due to creep induced from their self-weight and sustained loads.

For example, five composite slab samples were cast on KF70® [23] steel sheeting and five slabs cast on KF40® [23] steel sheeting, with spans of 3100 mm [50,51]. All slabs had the same cross-section (i.e., 1200-mm-wide and 150-mm-deep) and the moist curing was applied for six days from the day of casting. The samples were then placed in a simply-supported static configuration until 63 days of concrete age under self-weight only. After a period of 57 days of drying, the samples cast on KF70® [23] deck exhibited deflections in the range of 2.18–2.97 mm, while the samples cast on KF40® [23] had deflections within 2.72–3.33 mm (of the same order) already after 21 days of drying. These results highlighted the influence of shrinkage on the deflections of composite slabs. After 63 days from the casting date, sustained loads were applied on the specimens and these ranged from 0 (only self-weight) to 9.5 kN/m.

Table 2. Long-term tests of simply-supported composite slabs.

Ref.	Sample ID	f_c' [1] [MPa]	w_{sus} [1] [kN/m]	t_0 [1] [Days]	t_k [1] [Days]	L (l_0) [1] [mm]	b [1] [mm]	D [1] [mm]	Profiled Steel Sheeting	Remarks
[16]	CS1 CS2	27.3	0	15	119	3300 (3000)	900	180	Condeck HP® [21]	
	SS1 SS2	27.3	0	15	119	3300 (3000)	900	180	No	Solid slab [2]
[18]	CS-120 CS-180	29	4.5 9.0	28	268	3300 (3000)	510	120 180	DW-65-510-170	
	CS-120-SH CS-180-SH	29	0	28	268	3300 (3000)	510	120 180	DW-65-510-170	
[50]	1LT-70-0 2LT-70-3 3LT-70-3 4LT-70-6 5LT-70-8	28	0 4.1 4.1 7.2 7.3 9.5	64	242 242 242 242 196 242	3300 (3100)	1200	150	KF70® [23]	
	6LT-40-0 7LT-40-3 8LT-40-3 9LT-40-6 10LT-40-6	35.5	0 4.1 4.1 7.7 7.7	64	205	3300 (3100)	1200	150	KF40® [23]	
[52]	S1	31.1	2.1	8	134	3200 (3000)	918	125	MD55	
[14]	SS CK PF	33.7	0	8	239	7200 (6000)	900	180	No Condeck HP® [21] PrimeForm® [22]	Solid slab [2]
[54]	CK1 CK2 CK3 CK4	41.5	0	7	90	7200 (6000)	–	180	Condeck HP® [21]	
	CK5 CK6	41.5	0	7	90	8650 (7450)	–	225	Condeck HP® [21]	
[53]	SS1 SS2 SS3	32	0	14	267	3200 (3000)	634	120	Condeck HP® [21]	

Note: [1] f_c' is the measured compressive strength of the concrete; w_{sus} is the sustained uniformly distributed load; t_0 and t_k are the time of first loading and the time at the end of the long-term test, respectively; L, l_0, b, and D are the total length, clear span, width, and thickness of the samples, respectively. [2] Top and bottom surfaces exposed to the environment.

Long-term results for 119 days of composite slabs prepared with different amounts of reinforcement ratios were reported in [16] together with the measurements of two reinforced concrete slab samples prepared with amounts of steel reinforcement that were equivalent to one adopted in the companion composite slabs. This selection of reinforcement aimed at differentiating between the role of non-symmetric steel reinforcement specified in a slab to the one of the non-uniform shrinkage gradients. All slabs were 3300-mm-long and two composite slabs were cast on Stramit Condeck HP® [21] steel sheeting with the propped condition. All samples were subjected to moist curing until 15 days from the day of casting. They were then placed in a simply-supported static configuration and subjected to their self-weight only. The composite slabs were allowed to dry only from the top surfaces, whereas the reinforced concrete slabs were allowed to dry from both top and bottom surfaces. These tests highlighted the role played by the non-uniform shrinkage gradient in influencing the long-term response. The companion composite and reinforced concrete slab samples

exhibited different deflections even in the cases in which symmetric steel reinforcement was specified. In this case, the composite specimen underwent higher deflections than the reinforced concrete sample by about 54% and this difference was simply attributed to the non-symmetric drying conditions (as these companion samples possessed similar amounts of symmetric reinforcement). Similar considerations were also drawn for the companion specimens without top reinforcement while in this case the differences in deflections were even greater.

Table 3. Long-term tests of two-span continuous composite slabs.

Ref.	Sample ID	f_c' [1]	w_{sus} [1]	t_0 [1]	t_k [1]	L (l_0) [1]	b [1]	D [1]	Steel Sheeting
		[MPa]	[kN/m]	[Days]	[Days]	[mm]	[mm]	[mm]	
[19]	CCS-NAC-L CCS-RAC-L CCS-RAC-SH	57.5 47.4 47.4	4.5 4.5 0	28	500	6300 (6000)	510	120	DW-65
[53]	CS1 CS2 CS3	32	0	14	267	6200 (6000)	634	120	Condeck HP® [21]
[55]	CLT-70-0 CLT-70-3 CLT-70-6	36.7	0 3.72 6.72	28	376	6900 (6700)	1200	150	KF70® [23]
[56]	L1 L2 L3 L4 L5 L6 L7 L8 L9 L10 L11 L12 L13 L14 L15 L16	34.8 34.8 34.8 34.8 36.2 35.8 33.8 34.6 34.6 34.6 34.6 37.1 37.1 37.1 35.8 36.2	0	7	97	6300 (6000)	1200	150	ComFlor® 80 [57]
[58]	Slab 1 Slab 2 Slab 3 Slab 4	20	11.8 11.8 9.5 9.5	7	228 228 903 903	4600	914	150 150 125 125	Corrugated steel sheeting

Note: [1] f_c' is the measured compressive strength of the concrete; w_{sus} is the sustained uniformly distributed load; t_0 and t_k are the time of first loading and the time at the end of the long-term test, respectively; L, l_0, b, and D are the total length, clear span, width, and thickness of the samples, respectively.

Time-dependent experimental results of one-way simply-supported composite slabs made of recycled aggregate concrete with different thicknesses and loading conditions have been reported in [18,20]. Four simply-supported composite slabs having 3300-mm length and 510-mm width were cast on DW-65-510-170 steel deck. Slabs possessed two different thicknesses of 120 and 180 mm, and were subjected to different sustained loading conditions that ranged between 0 and 9.0 kN/m. The long-term tests were monitored for 268 days from the day of casting.

Reference [14] presented the long-term response of three simply-supported post-tensioned slabs, i.e., two samples were cast on profiled steel sheeting Condeck HP [21] and PrimeForm [22] and one specimen was prepared with a solid concrete slab. All samples were 7200-mm-long and had identical cross-section with 900-mm width and 180-mm depth.

The prestressing forces were applied in two stages at day 2 and day 7 from the day of casting, and subsequently, all slabs were unpropped to place them in simply-supported conditions. The long-term behavior was induced by shrinkage effects and by creep induced by the slab self-weight. The tests were monitored for a period of 239 days. The post-tensioned slab prepared with the solid slab (exposed to dry from both sides) experienced less than one-fifth of the deflection of the post-tensioned composite slabs (sealed at the bottom of the slab by the presence of the profiled steel sheeting). These comparisons highlighted the importance of accounting for the influence of shrinkage gradients when predicting deflections in composite slabs.

Six post-tensioned simply-supported composite samples cast with different dimensions, number of prestressing strands, continuity of the steel sheeting and curing conditions were presented in [54]. Four of the slabs were 7200-mm-long, and the other two were 8650-mm-long. The slab thicknesses varied between 180 and 225 mm.

All slabs were wet cured for 7 days from the day of casting and prestressing were completed by two stages at day 2 and day 6 from the day of casting. All samples were then placed in a simply-supported static configuration. The specimens exhibited similar long-term deflections except the one covered with curing compound after casting. The latter sample (i.e., cast with curing compound) exhibited half of the time-dependent deflections measured for the other post-tensioned composite specimens.

In a recent study, the influence of specifying different drying conditions on the time-dependent deflections of simply-supported composite slabs was presented in [53]. All slabs had a length of 3200 mm and were 634-mm-wide and 120-mm-deep. Those drying conditions of composite slabs were considered to replicate different scenarios that take place during building construction. For this purpose, three drying conditions were considered: (i) The top surface of one composite slab was sealed after casting; (ii) a second sample was sealed on its top surface after 37 days from casting to reflect the scenario in which a slab is sealed by floor finishes or by other treatments during construction; and (iii) the top surface of the third sample was left exposed for drying. The long-term measurements recorded for these specimens are illustrated in Figure 5.

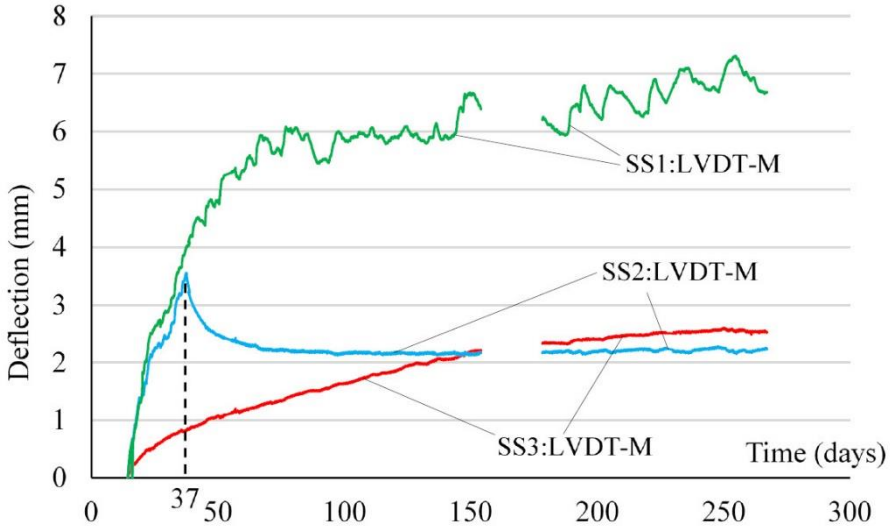

Figure 5. Mid-span deflections measured for simply-supported samples (LVDT-M = mid-span deflection) [53].

3.2. Continuous Composite Slabs

A number of continuous composite slabs have been tested to date to evaluate their long-term response as depicted in Table 3.

Two-span continuous composite concrete slabs having 6300 mm of total length were cast on ComFlor 80 [57] steel deck with similar cross-section of 150 by 1200 mm [56]. In reference [56], sixteen composite slabs were monitored over time and they exhibited 4

to 7 times higher long-term deflections after 90 days of drying than their instantaneous deflections under only self-weight. In this experimental work, different bonding between concrete and steel deck were created by the presence of embossments and grease, and different reinforcement ratios were adopted using mesh reinforcements, reinforcement bars and steel fibers. All samples were moist cured for 7 days from the day of casting.

Long-term deflections of the three continuous composite slabs with 6900 mm total length over two spans were monitored for 376 days [55,59]. All three slabs had the same cross-section with 150-mm thickness and 1200-mm width. These were cast on KF70® [23] steel sheeting that was supported on the floor during casting. The slabs were moist cured for 28 days from the day of casting and they were then subjected to different levels of sustained loading.

Three continuous composite slabs with 6300-mm total length over two-span and consisting of same cross-section of 510-mm-wide and 120-mm-deep were cast on DW-65 steel sheeting without propping. One of the slabs was prepared with natural aggregate, while the other two samples were made of recycled aggregate concrete. All slabs were wet cured for 6 days from the day of casting and subsequently monitored for their long-term responses for a period of 500 days [19].

Cracking over the interior support of two-span continuous composite slabs occurred in the specimens reported in [55,59] over time due to shrinkage. After 376 days from casting, maximum crack widths recorded in the continuous slabs were about 0.2, 0.3, and 0.6 mm for the samples subjected to 0, 3.72, and 6.72 kN/m, respectively. Reference [19] confirmed the role played by non-uniform shrinkage effects when considering cracking.

The occurrence of shrinkage influences the bending moment distribution and affects the magnitude of the negative moment over interior supports in the continuous static configurations [55,59]. This behavior was also observed experimentally in [19]. The composite slabs made with recycled aggregate concrete experienced higher deflection than those prepared natural concrete because of the higher shrinkage exhibited by the recycled aggregate concrete [19]. Negligible end slips between steel sheeting and concrete were observed under service load [55,59].

The time-dependent response of composite slabs cast with either steel mesh or polypropylene/poly-ethylene blend fibers were compared in [58]. As part of this experimental program, four 914-mm-wide and 4600-mm-long continuous slabs were cast on corrugated steel sheet with two different thicknesses (i.e., thicknesses of 125 and 150 mm) and wet cured for 7 days. After curing, slabs were placed in continuous support condition and subjected to their self-weight until 28 days from the day of casting. Thereafter, two 150-mm and two 125-mm thick slabs were uniformly loaded with 11.8 and 9.5 kN/m, respectively, and monitored for their long-term behavior. The ratio between the instantaneous deflections and long-term deflections of the slabs varied between 1.35 to 1.51. The ratio between the short-term crack widths and the long-term crack widths of these samples varied between 2.00 to 2.85.

Recent experimental measurements carried out on three identical continuous slabs that varied only in their exposure conditions for drying was reported in [53]. Three 6200-mm-long continuous slabs were cast on Condeck HP® [21] Profiled sheeting under propped conditions. The slabs possessed identical dimensions of 634-mm width and 120-mm depth and were wet cured for 7 days. The slabs were subjected to their self-weight from 14 days of concrete age and monitored for 267 days from the day of casting. Measured mid-span deflections recorded at the mid-spans of the two end spans are shown in Figure 6. The top surface of sample CS3 was sealed with a plastic sheet after casting and maintained the lowest increases in shrinkage deflections because its drying component was affected. A second sample, i.e., specimen CS2, was maintained exposed to dry until 37 days from casting, after which its top surface was sealed. This produced a change in the composite response that led to a slight decrease in deflections. A third sample, denoted as CS1 was kept exposed for drying for the entire long-term test duration. These tests highlighted the

role of exposure drying conditions on the time-dependent deflections of composite slabs to represent typical sealing conditions that could occur during the construction of a floor slab.

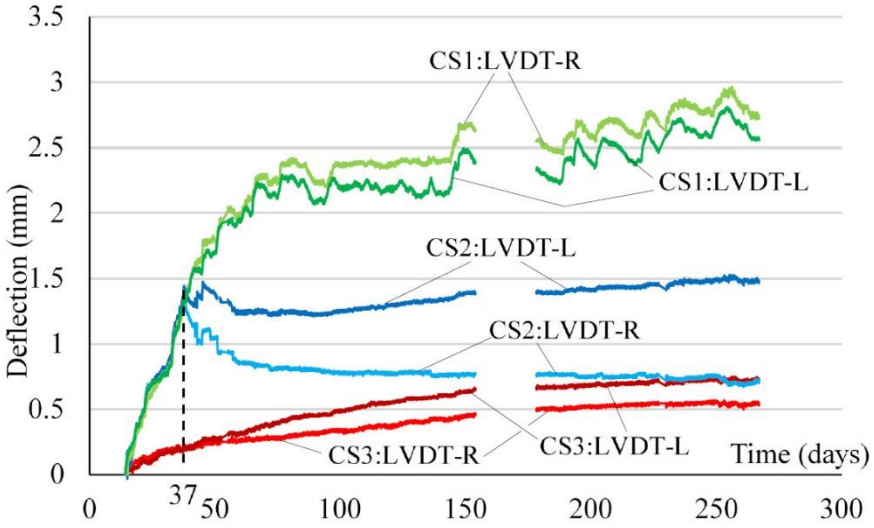

Figure 6. Mid-span deflections measured for the continuous specimens (LVDT-L = mid-span deflection of left span; LVDT-R = mid-span deflection of right span) [53].

4. Time-Dependent Modelling of Composite Slabs

4.1. Numerical Model

The time-dependent behavior of composite slabs has been commonly represented by means of full shear interaction theory [7,8,60,61] that assumed relative movement to occur between the slab and the profiled steel sheeting. Based on the age-adjusted effective modulus method (AEMM), reference [62] adopted a constant uniform shrinkage profile through the thickness of the composite slab.

A closed-form solution to calculate the deflections and stresses in one-way composite steel–concrete slabs over time was proposed in [63,64]. The formulation was based on the principle of virtual work and the model can account for different shrinkage profiles, including non-uniform shrinkage distributions such as those that can occur in composite slabs. Other methods of analysis to capture the composite time-dependent response accounting for shrinkage gradients were presented in [17,55,59,65,66]. In [17], the influence of non-uniform shrinkage gradients on the deflection response was included in the analysis by assuming the composite slab cross-section to be discretized into several layers. In this study, four different shrinkage profiles were considered and these consisted of a uniform shrinkage profile, a triangular shrinkage profile, a bilinear shrinkage profile and a parabolic shrinkage profile. Full shear interaction was also assumed between the concrete and profiled steel sheeting.

The long-term behavior of post-tensioned composite slabs based on the Euler-Bernoulli beam theory was presented in [14]. Long-term analyses were performed by means of the step-by-step procedure in which the time domain is discretized in different time steps and is widely used in the long-term predictions of concrete structures as, for example, outlined in [8]. Measured shrinkage gradients that occurred through the thickness of the slab were considered to calculate the long-term deflection of the composite slabs. Comparisons were made between experimental and calculated deflections. With the same beam assumptions, a non-linear solution strategy was considered in [18,19] based on the formulations described in [67]. Based on their experimental results, full interaction between concrete and steel sheeting were considered in the analysis. Linear shrinkage gradients were assumed to occur through the thickness of the composite slab to account for the non-uniform shrinkage strains.

The non-uniform shrinkage effects on the time-dependent behavior of composite and post-tensioned slabs were presented in [68]. A hygro-thermo-chemical-mechanical model has been proposed to calculate the more refined non-uniform shrinkage profiles from the temperature and relative humidity distribution through the thickness of the composite slab [69]. The time-dependent response of the composite slab was then obtained from the cross-sectional analysis introduced in [8]. In this study, measured long-term deflections of composite slabs presented in [54] were used to validate the numerical predictions. Comparisons with measured deflections are shown in Figure 7. For this purpose, three different shrinkage profiles were considered and included (Figure 7): (i) a uniform shrinkage profile typically used in reinforced concrete solid slabs; (ii) a linearly varying shrinkage gradient that was specified in accordance with the specifications of the Australian composite guidelines [12,13] (and suitable for routine design)—this case is referred to as 'simplified approach' in Figure 7; and (iii) a shrinkage gradient that is determined from the hygro-thermo-chemical-mechanical model based on the inverse analysis procedure described in [69]. The comparisons between the numerical and experimental results highlighted the importance of accounting for the shrinkage gradients when estimating the long-term deflections of composite slabs and the ability of the hygro-thermo-chemical-mechanical model to capture the shrinkage gradient that occurred in the slab.

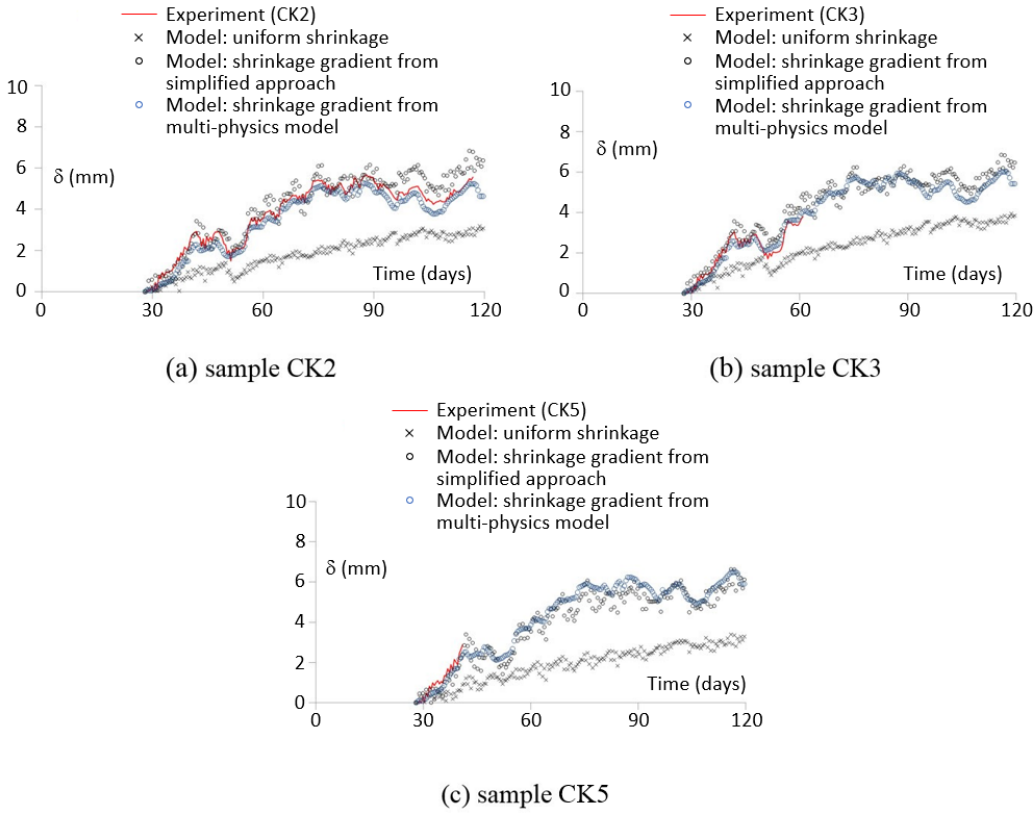

Figure 7. Experimental and numerical mid-span deflections considering different shrinkage profiles [68].

A non-linear thermo-mechanical finite element model developed in ABAQUS was presented in [70] to predict the long-term response of composite slabs.

4.2. Design Model

Different design models were proposed in the literature to capture the non-linear shrinkage gradients that develop in composite slabs.

Reference [65] presented a design expression to evaluate the shrinkage induced curvature that accounted for the influence of the following parameters: a factor that depends on

the profile of the steel sheeting; a parameter denoting the reinforcement ratio produced by the steel sheeting; the shrinkage strain induced at the top drying surface of the slab; and the total slab thickness. The authors also considered the cases of composite slabs cast on trapezoidal steel sheeting, for which they proposed some additional modification factors to be used in the calculations.

An expression for the shrinkage strain profile for a composite slab with steel sheeting was presented in [66]. This was written in terms of the following variables: the shrinkage strain at any height of the cross-section; the shrinkage strain calculated following available design codes over the time of interest; the steel sheeting profile; and for trapezoidal sheeting profiles, the ratio between a trough height and the slab thickness. A modification to the definition of the hypothetical thickness used in AS 3600-2009 [11] was proposed in [55] to account for the response of composite slabs.

The occurrence of the non-uniform shrinkage profile in composite slabs was considered in [18,19,70] and it was estimated to be taken as 1.2 and 0.2 times of the design shrinkage strain at the top and bottom surfaces of the slab, respectively [15,16]. Design shrinkage strains over time were predicted using concrete design specifications by considering the case of a solid slab with the same thickness as the composite slab and exposed to dry from both its top and bottom surfaces. The long-term predictions of the composite slab response have also been presented in [68] based on these shrinkage gradients.

A comprehensive design guideline for calculating the instantaneous and long-term deflections of composite slabs considering the non-uniform shrinkage profile through the slab thickness was presented in [12]. The instantaneous deflection was obtained from available design codes, whereas deflection due to creep was evaluated from the effective modulus method. The reference shrinkage strains over time were calculated following design guidelines [11], while adopting the hypothetical thickness equal to the thickness of the composite slab, and the gradient was assumed as the same gradient reported in [15,16]. This design procedure was adopted in AS/NZS 2327:2017 [13] under its simplified approaches for the calculation of the composite slab deflection.

5. Conclusions

Extensive research work has been carried out to date to define the ultimate behavior of composite slabs, whereas limited research has dealt with their long-term behavior. This paper presented a state-of-the-art review of research on the long-term behavior of composite slabs. Particular attention was given to the occurrence of the shrinkage gradient in composite steel–concrete slabs due to the presence of steel sheeting and its influence on the long-term response of the composite slabs in this paper. After presenting the key features related to the development of the shrinkage gradients in composite slabs, a review of experiments performed on simply-supported and continuous composite slab samples were presented to highlight the influence of the different factors considered in these studies, such as the use of different geometries, loading conditions, and drying conditions, and how these influenced the development of the shrinkage gradients on the long-term behavior of composite slabs. At the end of the paper, available theoretical and design models for the time-dependent behavior of composite slabs were introduced and discussed. The work reported in the literature highlighted the importance of accounting for the non-uniform shrinkage gradient when predicting long-term deflections induced by shrinkage effects. By neglecting the shrinkage gradient can lead to significant underestimations of the shrinkage-induced deflection. Tests performed in the literature highlighted how this effect is important for different arrangements of the steel reinforcement. Recent work has pointed out that the non-uniform shrinkage gradient can be significantly mitigated if the composite slab is sealed on its top surface soon after casting or curing. This condition could reflect the typical scenario that occurs in a construction site in which a building floor could be sealed by the application of floor finishes or treatments. Design guidelines to account for the non-uniform shrinkage gradient have already been incorporated in the Australian

composite specifications and are currently being considered for possible introduction by other international design standards.

Author Contributions: Conceptualization, M.M.R. and G.R.; methodology, M.M.R. and G.R.; data curation, M.M.R. and G.R.; writing—original draft preparation, M.M.R. and G.R.; writing—review and editing, M.M.R. and G.R. All authors have read and agreed to the published version of the manuscript.

Funding: This research received no external funding.

Institutional Review Board Statement: Not applicable.

Informed Consent Statement: Not applicable.

Data Availability Statement: Not applicable.

Conflicts of Interest: The authors declare no conflict of interest.

References

1. Oehlers, D.J.; Bradford, M.A. *Composite Steel and Concrete Structural Members: Fundamental Behaviour*; Elsevier: Amsterdam, The Netherlands, 1995. [CrossRef]
2. Oehlers, D.J.; Bradford, M.A. *Elementary Behaviour of Composite Steel and Concrete Structural Members*; Butterworth-Heinemann: Oxford, UK, 1999.
3. Nethercot, D. (Ed.) *Composite Construction*; CRC Press: Boca Raton, FL, USA, 2003. [CrossRef]
4. Johnson, R.P. *Composite Structures of Steel and Concrete*, 4th ed.; Wiley Blackwell: Hoboken, NJ, USA, 2018.
5. Collings, D. *Steel—Concrete Composite Buildings: Designing with Eurocodes*; Thomas Telford Ltd.: London, UK, 2010.
6. Taranath, B.S. *Structural Analysis and Design of Tall Buildings: Steel and Composite Construction*; CRC Press: Boca Raton, FL, USA, 2016.
7. Ghali, A.; Favre, R.; Elbadry, M. *Concrete Structures: Stresses and Deformations*, 3rd ed.; CRC Press: London, UK; New York, NY, USA, 2002. [CrossRef]
8. Gilbert, R.I.; Ranzi, G. *Time-Dependent Behaviour of Concrete Structures*, 1st ed.; Spon Press: London, UK, 2011. [CrossRef]
9. Ranzi, G.; Leoni, G.; Zandonini, R. State of the Art on the Time-Dependent Behaviour of Composite Steel–Concrete Structures. *J. Constr. Steel Res.* **2013**, *80*, 252–263. [CrossRef]
10. Bocciarelli, M.; Caldentey, A.P.; Cusatis, G.; Dezi, L.; Dönmez, A.A.; Di Luzi, G.; Geng, Y.; Gilbert, R.; Hewitt, J.; Jordán, J.; et al. *Time-Dependent Behaviour and Design of Composite Steel-Concrete Structures*; Ranzi, G., Ed.; International Association for Bridge and Structural Engineering (IABSE): Zurich, Switzerland, 2021. [CrossRef]
11. Standards Australia. *Australian Standard for Concrete Structures. AS 3600-2009*; Standards Australia: Sydney, Australia, 2009.
12. Ranzi, G. Service Design Approach for Composite Steel–Concrete Floors. *Proc. Inst. Civ. Eng. Struct. Build.* **2018**, *171*, 38–49. [CrossRef]
13. Australian/New Zealand Standard. *Composite Structures—Composite Steel-Concrete Construction in Buildings. AS/NZS 2327:2017*; Standards Australia: Sydney, Australia, 2017.
14. Ranzi, G.; Al-Deen, S.; Ambrogi, L.; Uy, B. Long-Term Behaviour of Simply-Supported Post-Tensioned Composite Slabs. *J. Constr. Steel Res.* **2013**, *88*, 172–180. [CrossRef]
15. Al-deen, S.; Ranzi, G. Effects of Non-Uniform Shrinkage on the Long-Term Behaviour of Composite Steel-Concrete Slabs. *Int. J. Steel Struct.* **2015**, *15*, 415–432. [CrossRef]
16. Al-Deen, S.; Ranzi, G.; Uy, B. Non-Uniform Shrinkage in Simply-Supported Composite Steel-Concrete Slabs. *Steel Compos. Struct.* **2015**, *18*, 375–394. [CrossRef]
17. Gilbert, R.I.; Bradford, M.A.; Gholamhoseini, A.; Chang, Z.-T. Effects of Shrinkage on the Long-Term Stresses and Deformations of Composite Concrete Slabs. *Eng. Struct.* **2012**, *40*, 9–19. [CrossRef]
18. Wang, Y.; Wang, Q.; Geng, Y.; Ranzi, G. Long-Term Behaviour of Simply Supported Composite Slabs with Recycled Coarse Aggregate. *Mag. Concr. Res.* **2016**, *68*, 1278–1293. [CrossRef]
19. Zhang, H.; Geng, Y.; Wang, Y.Y.; Wang, Q. Long-Term Behavior of Continuous Composite Slabs Made with 100% Fine and Coarse Recycled Aggregate. *Eng. Struct.* **2020**, *212*, 110464. [CrossRef]
20. Wang, Q.; Yang, J.; Patrick, B.; Zheng, A.; Shi, Y. Long-Term Shrinkage Behaviour of Steel-Concrete Composite Slabs with Recycled Coarse Aggregate. *IOP Conf. Ser. Earth Environ. Sci.* **2020**, *510*, 052028. [CrossRef]
21. Stramit. *Stramit Condeck HP, Composite Slab System, Product Technical Manual*; Stramit Corporation Property Limited: Queensland, Australia, 2012.
22. Stramit. *Stramit PrimeForm Left-Iniplace Formwork System, Product Technical Manual*; Stramit Corporation Property Limited: Banyo, Australia, 2011.
23. Fielders Australia. *Specifying Fielders–Kingflor–Composite Steel Formwork System Design Manual*; Fielders Australia Pty Ltd.: Marleston, Australia, 2008.

24. Bažant, Z.P.; Jirásek, M. Solid Mechanics and Its Applications. In *Creep and Hygrothermal Effects in Concrete Structures*; Springer: Dordrecht, The Netherlands, 2018; Volume 225. [CrossRef]
25. Jiang, Z.; Sun, Z.; Wang, P. Autogenous Relative Humidity Change and Autogenous Shrinkage of High-Performance Cement Pastes. *Cem. Concr. Res.* **2005**, *35*, 1539–1545. [CrossRef]
26. Hu, S.; Wu, J.; Yang, W.; Lu, L.; He, Y. Relationship between Autogenous Deformation and Internal Relative Humidity of High-Strength Expansive Concrete. *J. Wuhan Univ. Technol. Sci. Ed.* **2010**, *25*, 504–508. [CrossRef]
27. Zhang, J.; Dongwei, H.; Wei, S. Experimental Study on the Relationship between Shrinkage and Interior Humidity of Concrete at Early Age. *Mag. Concr. Res.* **2010**, *62*, 191–199. [CrossRef]
28. Jun, Z.; Dongwei, H.; Haoyu, C. Experimental and Theoretical Studies on Autogenous Shrinkage of Concrete at Early Ages. *J. Mater. Civ. Eng.* **2011**, *23*, 312–320. [CrossRef]
29. Wei, Y.; Huang, J.; Liang, S. Measurement and Modeling Concrete Creep Considering Relative Humidity Effect. *Mech. Time-Dependent Mater.* **2020**, *24*, 161–177. [CrossRef]
30. Zhang, J.; Gao, Y.; Han, Y.; Sun, W. Shrinkage and Interior Humidity of Concrete under Dry–Wet Cycles. *Dry. Technol.* **2012**, *30*, 583–596. [CrossRef]
31. Parrott, L.J. Moisture Profiles in Drying Concrete. *Adv. Cem. Res.* **1988**, *1*, 164–170. [CrossRef]
32. Parrott, L.J. Factors Influencing Relative Humidity in Concrete. *Mag. Concr. Res.* **1991**, *43*, 45–52. [CrossRef]
33. Kim, J.-K.; Lee, C.-S. Moisture Diffusion of Concrete Considering Self-Desiccation at Early Ages. *Cem. Concr. Res.* **1999**, *29*, 1921–1927. [CrossRef]
34. Grasley, Z.C.; Lange, D.A.; D'Ambrosia, M.D. Internal Relative Humidity and Drying Stress Gradients in Concrete. *Mater. Struct.* **2006**, *39*, 901–909. [CrossRef]
35. Jiang, Z.; Sun, Z.; Wang, P. Internal Relative Humidity Distribution in High-Performance Cement Paste Due to Moisture Diffusion and Self-Desiccation. *Cem. Concr. Res.* **2006**, *36*, 320–325. [CrossRef]
36. Amba, J.C.; Balayssac, J.P.; Détriché, C.H. Characterisation of Differential Shrinkage of Bonded Mortar Overlays Subjected to Drying. *Mater. Struct.* **2010**, *43*, 297–308. [CrossRef]
37. Holmes, N.; West, R.P. Enhanced Accelerated Drying of Concrete Floor Slabs. *Mag. Concr. Res.* **2013**, *65*, 1187–1198. [CrossRef]
38. Holmes, N. *Moisture Movement in Concrete During Drying*; University of Dublin: Dublin, Ireland, 2009.
39. Ramseyer, C.; Shadravan, S.; Gorman, P.; Santamaria, C.R. *Dimensional Stability of Concrete Slabs on Grade*; Oklahoma Transportation Center: Midwest City, OK, USA, 2012.
40. Bocciarelli, M.; Ranzi, G.; Rahman, M. A Hygro-Thermo-Chemical-Mechanical Model for the Shrinkage Prediction in Composite Steel-Concrete Floors. In Proceedings of the 28th Biennial National Conference of the Concrete Institute of Australia, Adelaide, Australia, 22–25 October 2017; pp. 1–10.
41. Azenha, M.; Leitão, L.; Granja, J.L.; de Sousa, C.; Faria, R.; Barros, J.A.O. Experimental Validation of a Framework for Hygro-Mechanical Simulation of Self-Induced Stresses in Concrete. *Cem. Concr. Compos.* **2017**, *80*, 41–54. [CrossRef]
42. Azenha, M.; Granja, J.L. Monitoring and Simulating Humidity Profiles in Concrete Elements during Drying. In Proceedings of the International RILEM Conference on Materials, Systems and Structures in Civil Engineering Conference segment on Moisture in Materials and Structures, Lyngby, Denmark, 22–24 August 2016; pp. 115–124.
43. Choi, S.; Won, M.C. Thermal Strain and Drying Shrinkage of Concrete Structures in the Field. *ACI Mater. J.* **2010**, *107*, 498–507. [CrossRef]
44. Zhang, J.; Huang, Y.; Qi, K.; Gao, Y. Interior Relative Humidity of Normal- and High-Strength Concrete at Early Age. *J. Mater. Civ. Eng.* **2012**, *24*, 615–622. [CrossRef]
45. Pour-ghaz, M.; Spragg, R.; Weiss, J. Moisture Profiles and Diffusion Coefficients in Mortars Containing Shrinkage Reducing Admixtures. In Proceedings of the International RILEM Conference on Use of Superabsorbent Polymers and Other New Additives in Concrete, Lyngby, Denmark, 15–18 August 2010; pp. 197–206.
46. Zhou, J.; Chen, X.; Zhang, J.; Wang, Y. Internal Relative Humidity Distribution in Concrete Considering Self-Desiccation at Early Ages. *Int. J. Phys. Sci.* **2011**, *6*, 1604–1610. [CrossRef]
47. Zhang, J.; Gao, Y.; Han, Y. Interior Humidity of Concrete under Dry-Wet Cycles. *J. Mater. Civ. Eng.* **2012**, *24*, 289–298. [CrossRef]
48. Wei, Y.; Liang, S.; Gao, X. Numerical Evaluation of Moisture Warping and Stress in Concrete Pavement Slabs with Different Water-to-Cement Ratio and Thickness. *J. Eng. Mech.* **2017**, *143*, 04016111. [CrossRef]
49. Wei, Y.; Gao, X.; Hansen, W. Influential Depth by Water Absorption and Surface Drying in Concrete Slabs. *Transp. Res. Rec. J. Transp. Res. Board* **2013**, *2342*, 76–82. [CrossRef]
50. Gholamhoseini, A.; Gilbert, R.I.; Bradford, M.A.; Chang, Z.T. Long-Term Deformation of Composite Concrete Slabs under Sustained Loading. In Proceedings of the From Materials to Structures: Advancement Through Innovation—Proceedings of the 22nd Australasian Conference on the Mechanics of Structures and Materials, ACMSM, Sydney, Australia, 11–14 December 2012; pp. 67–72.
51. Gholamhoseini, A. Modified Creep and Shrinkage Prediction Model B3 for Serviceability Limit State Analysis of Composite Slabs. *Int. J. Adv. Struct. Eng.* **2016**, *8*, 87–101. [CrossRef]
52. Oliveira, L.A.M.; Borghi, T.M.; Rodrigues, Y.O.; El Debs, A.L.H.D.C. Assessment of Design Codes for the In-Service Behaviour of Steel-Concrete Composite Slabs. *IBRACON Struct. Mater. J.* **2021**, *14*, e14501. [CrossRef]

53. Ranzi, G.; Frigerio, G.; Vallati, O. Long-Term Experiments on Composite Slabs Exposed to Different Surface Drying Conditions. In Proceedings of the 16th East Asian-Pacific Conference on Structural Engineering and Construction, Brisbane, Australia, 3–6 December 2019; Springer Science+Business Media: Brisbane, Australia, 2019. [CrossRef]
54. Ranzi, G.; Ostinelli, A.; Uy, B. An Experimental Study on the Shrinkage and Ultimate Behaviour of Post-Tensioned Composite Slabs. In Proceedings of the 22nd Australasian Conference on the Mechanics of Structures and Materials (ACMSM22), Sydney, Australia, 11–14 December 2012; Samali, A.S., Ed.; CRC Press: Boca Raton, FL, USA; Sydney, Australia, 2013; pp. 339–344.
55. Gholamhoseini, A.; Gilbert, R.I.; Bradford, M.A. Long-Term Deformations in Continuous Composite Concrete Slabs. *Aust. J. Struct. Eng.* **2016**, *17*, 197–212. [CrossRef]
56. Gholamhoseini, A.; Khanlou, A.; MacRae, G.; Scott, A.; Hicks, S.; Leon, R. An Experimental Study on Strength and Serviceability of Reinforced and Steel Fibre Reinforced Concrete (SFRC) Continuous Composite Slabs. *Eng. Struct.* **2016**, *114*, 171–180. [CrossRef]
57. Steel & Tube Holdings Ltd. *Product Guide, ComFlor 80, Composite Floor Decking*; Steel & Tube Holdings Ltd.: Auckland, New Zealand, 2016.
58. Altoubat, S.; Rieder, K.A.; Junaid, M.T. Short- and Long-Term Restrained Shrinkage Cracking of Fiber Reinforced Concrete Composite Metal Decks: An Experimental Study. *Mater. Struct. Constr.* **2017**, *50*, 1–15. [CrossRef]
59. Gholamhoseini, A.; Gilbert, R.I.; Bradford, M. Long-Term Behavior of Continuous Composite Concrete Slabs with Steel Decking. *ACI Struct. J.* **2018**, *115*, 439–449. [CrossRef]
60. Gilbert, R.I. *Time Effects in Concrete Structures*; Elsevier Science Publishers: Amsterdam, The Netherlands, 1988.
61. Gilbert, R.I. Time-Dependent Analysis of Composite Steel-Concrete Sections. *J. Struct. Eng.* **1989**, *115*, 2687–2705. [CrossRef]
62. Uy, B. Long-Term Service-Load Behaviour of Simply Supported Profiled Composite Slabs. *Proc. Inst. Civ. Eng. Struct. Build.* **1997**, *122*, 193–208. [CrossRef]
63. Bradford, M.A. Generic Modelling of Composite Steel–Concrete Slabs Subjected to Shrinkage, Creep and Thermal Strains Including Partial Interaction. *Eng. Struct.* **2010**, *32*, 1459–1465. [CrossRef]
64. Bradford, M.A.; Gilbert, R.I.; Zeuner, R.; Brock, G. Shrinkage Deformations of Composite Slabs with Open Trapezoidal Sheeting. *Procedia Eng.* **2011**, *14*, 52–61. [CrossRef]
65. Gilbert, R.I. Time-Dependent Stiffness of Cracked Reinforced and Composite Concrete Slabs. *Procedia Eng.* **2013**, *57*, 19–34. [CrossRef]
66. Gholamhoseini, A.; Gilbert, R.I.; Bradford, M.; Chang, Z.-T. Time-Dependent Deflection of Composite Concrete Slabs. *ACI Struct. J.* **2014**, *111*, 765–775. [CrossRef]
67. Ranzi, G.; Gilbert, R.I. *Structural Analysis: Principles, Methods and Modelling*; CRC Press: New York, NY, USA, 2015. [CrossRef]
68. Bocciarelli, M.; Ranzi, G. Evaluation of Shrinkage-Induced Deflections of Composite Slabs with a Simplified Design Approach and a Hygro-Thermo-Chemical-Mechanical Model. In Proceedings of the 25th Australasian Conference on the Mechanics of Structures and Materials (ACMSM25), Brisbane, Australia, 4−7 December 2018; Wang, C.M., Ho, J.C.M., Kitipornchai, S., Eds.; Springer: Singapore; Brisbane, Australia, 2018. [CrossRef]
69. Bocciarelli, M.; Ranzi, G. Identification of the Hygro-Thermo-Chemical-Mechanical Model Parameters of Concrete through Inverse Analysis. *Constr. Build. Mater.* **2018**, *162*, 202–214. [CrossRef]
70. Wang, Q.; Yang, J.; Liang, Y.; Zhang, H.; Zhao, Y.; Ren, Q. Prediction of Time-Dependent Behaviour of Steel–Recycled Aggregate Concrete (RAC) Composite Slabs via Thermo-Mechanical Finite Element Modelling. *J. Build. Eng.* **2020**, *29*, 101191. [CrossRef]